Theoretical and Applied Climatology (2022) 148:1513–1527
https://doi.org/10.1007/s00704-022-04013-8

ORIGINAL PAPER

Coupling analysis of surface runoff variation with atmospheric teleconnection indices in the middle reaches of the Yangtze River

Wenyu Wang[1] · Peng Yang[1] · Jun Xia[2] · Shengqing Zhang[1] · Wei Cai[1]

Received: 10 May 2021 / Accepted: 5 March 2022 / Published online: 18 March 2022

Abstract

Changes in surface runoff and its coupling relationship with atmospheric circulation have been an ongoing focus of climate change research. In this study, the Mann–Kendall test, Pettitt test, and quantile regression were used to analyze changes in surface runoff in the middle reaches of the Yangtze River Basin (MYRB) during 1902–2014 based on the global runoff reconstruction (GRUN) dataset. In addition, cross wavelet analysis was used to analyze the coupling relationships between four teleconnection indices from the National Oceanic and Atmospheric Administration (NOAA) website (i.e., East Central Tropical Pacific SST (El Niño 3.4), Pacific Decadal Oscillation (PDO), Eastern Pacific/North Pacific Oscillation Index (EP/NP) and multivariate ENSO Index (MEI V2)), and monthly average surface runoff series in the MYRB. The study produced several important results: (1) Trends in the annual surface runoff, from 1902 to 2014, in the MYRB have changed significantly, with the longest and most significant upward trend occurring from 1987 to 2000. (2) The annual series surface runoff mutation years varied across the MYRB (e.g., surface runoff in the central region changed abruptly around 1918, whereas surface runoff in the northern and southern regions changed abruptly around 2000). (3) Significant correlations ($P < 0.05$) between the surface runoff in the MYRB and the four representative teleconnection indices (e.g., El Niño 3.4, PDO, EP/NP, and MEI V2) indicate that surface runoff has been strongly linked to the indices. The significance of this study lies in its revelation of relationships between water resources system changes and climate change.

Keywords Surface runoff changes · Yangtze River · Quantile regression · Cross wavelet

1 Introduction

Due to climate change, the melting of ice sheets has accelerated, leading to global sea level rise (Trusel et al. 2018), and extreme weather events have led to severe droughts, floods, and storms (Kalisa et al. 2021). Thus, the impacts of climate change on environments are attracting increasing attention (Chen et al. 2019). Such changes affect not only precipitation and temperature but also the normal operation of the global water cycle (Meng et al. 2019).

Surface runoff is an extremely significant part of the global water cycle, and any changes in it can affect human production and life (Ding et al. 2014). For example, recently, in mainland China, biological habitat reduction, frequent droughts and floods, and environmental deterioration along dried rivers have seriously affected human safety and economic development, with immeasurable losses (Ding et al. 2014). In recent decades, under global climate change and human activities, alternating droughts and floods have occurred frequently in China, resulting in intense impacts on water and food security (Shan et al. 2018). Terrestrial water storage can also affect the hydrological cycle (Pokhrel et al. 2021). Prior studies have found that ocean circulation changes, as measured by the teleconnection indices (e.g., East Central Tropical Pacific SST (El Niño 3.4), Pacific Decadal Oscillation (PDO)), also seriously impact surface runoff in the East Asian monsoon region. For example, the Normalized Difference Vegetation Index (NDVI) and the El Niño–Southern Oscillation (ENSO) circulation index were found to be the factors most correlated with surface runoff, and the combined NDVI–TMP and ENSO–PDO had even stronger relations with surface runoff (Yang et al. 2021).

✉ Peng Yang
806680403@qq.com

[1] School of Geography and Information Engineering, China University of Geosciences, Wuhan 430074, China

[2] State Key Laboratory of Water Resources and Hydropower Engineering Science, Wuhan University, Wuhan 430000, China

Therefore, to obtain a better understanding of the impact of climate change on surface runoff, it is important to study the relationships between surface runoff changes and teleconnection indices.

Recently, many studies have examined changes in surface runoff as well as the correlation between surface runoff and atmospheric circulation. Surface runoff is mainly affected by climate change and human activities (Farsi and Mahjouri 2019). At the same time, surface runoff impacts human society. For example, Resende et al. (2019) showed that an increase in extreme surface runoff would affect corn production in the Parana region of Brazil. In previous studies, a variety of trend testing methods (e.g., the Mann–Kendall test, Pettitt test, and quantile regression) were used to analyze changes in surface runoff (e.g., Zhang et al. 2014; Papacharalampous et al. 2018; Grinsted et al. 2004). The advantages of such studies lie in their ability to use a variety of scientific methods to analyze the characteristics of surface runoff changes, the impacts of these changes, and their relationships with other environmental factors quantitatively and from different perspectives. However, although a variety of methods to detect surface runoff trends and verify the reliability of the test results have been used, few studies have sought to analyze the teleconnection between atmospheric circulation and regional surface runoff. Furthermore, the influence of the underlying surface on runoff is frequently ignored, preventing comprehensive evaluation of the surface runoff.

The Yangtze River Basin (YRB) is among the river basins with the highest drought and flood risk in the world (Ye et al. 2017). Moreover, as the middle and lower reaches of the Yangtze River Basin (MYRB) are among the fastest-growing regions in China, the area is especially vulnerable to droughts and floods (Zhang et al. 2008). Although both natural and anthropogenic factors impact surface runoff in the YRB, climate change is the main cause of its seasonal changes (Chai et al. 2019). Under the influence of intensive human activities, the surface runoff in the YRB has a complex history (Kuang et al. 2014). The construction of the Three Gorges Dam, for example, altered downstream hydrological conditions and so directly affected the exchange of water between Dongting Lake and the Yangtze River (Sun et al. 2012). Meanwhile, excessive development and land utilization in the YRB have led to problems, such as declining ecosystem services (Chen 2020). The YRB should be used efficiently and protected effectively according to the characteristics of the country and basin (Wang et al. 2013). Regional studies such as those mentioned above can analyze trends in YRB surface runoff over multiple time scales, examine the ecological impacts of changes in surface runoff, and explore relationships between such changes and the environment. However, the methods used to detect surface runoff trends have been relatively simple, and few studies have included analyses of the impacts of atmospheric circulation and underlying surfaces. Therefore, this study had the following objectives: (1) analyze long-term surface runoff changes from 1902 to 2014 based on the global runoff reconstruction (GRUN) dataset using the Mann–Kendall trend test, Pettitt test, and quantile regression methods and (2) study the coupling relationship between teleconnection indices and surface runoff using cross wavelet analysis.

2 Study area

The MYRB between Yichang and Hukou comprises the main axis of the Yangtze River Economic Zones and is an important region of China (Yuan et al. 2012). The MYRB in central China comprises three sub-basins: the Dongting Lake Basin, Han River Basin, and Yichang–Hukou reaches (Zheng et al. 2021). Figure 1 shows the topography and water system distribution of the study area.

Most of the MYRB terrain is in the third step (the plain) of the three major topographic steps in China, whereas a small part is in the second step. The eastern part of the region is relatively low, whereas the western part is higher (Liu 2008). The overall elevation range is approximately 100 m, and there is little fluctuation (Chen et al. 2020). The area is subtropical, with an annual precipitation of 1000 to 1400 mm (Zhao and Mo 2020). The annual average temperature is 16–18 °C, the active cumulative temperature above 10 °C, and the duration of such days has generally increased significantly (Li 2021). Rice is cultivated in most areas under a triple cropping system. The area is suitable for many types

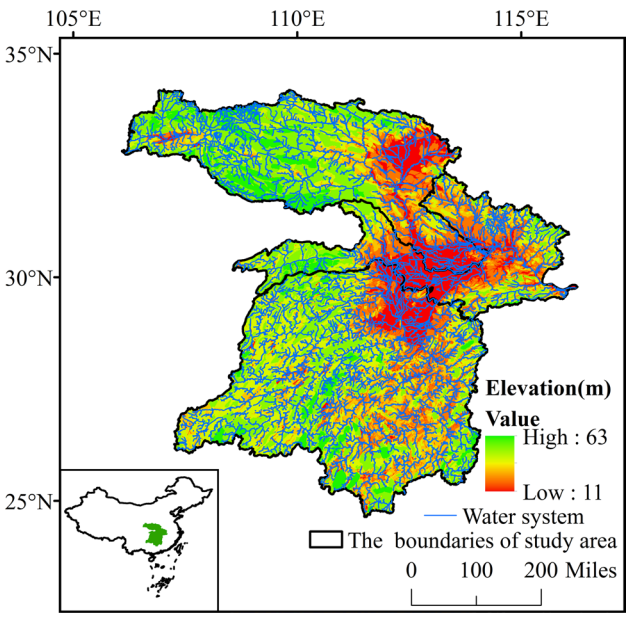

Fig. 1 Study area

of crops, especially those with a short growth cycle and long growth period (Su et al. 2005). The MYRB has the highest density of river networks in mainland China; these include natural water systems and lakes and artificial crisscrossing channels (Lai et al. 2014).

3 Materials and methods

3.1 Materials

3.1.1 Surface runoff data

The surface runoff data used in the study were from the GRUN (Do et al. 2018; Gudmundsson et al. 2017), which was not the measurement data from the gauging stations. This dataset contains global monthly time series surface runoff from 1902 to 2014. The spatial resolution of the dataset using the WGS1984 coordinate system is 0.5°. The dataset can be obtained from https://www.research-collection.ethz.ch/handle/20.500.11850/324386?show=full. Using the Global Soil Moisture Project Phase 3 (GSWP3) meteorological forcing dataset, historical precipitation and temperature data were used to predict monthly surface runoff (Kim 2015). The dataset reproduces well the dynamics of surface runoff on a global scale, and the accuracy of this reconstruction was assessed by cross-validation and compared with independent discharge observation datasets from large watersheds (Ghiggi et al. 2019). Its agreement with streamflow observations is on average better than the combination of 13 state-of-the-art global hydrological model surface runoff simulations (Ghiggi et al. 2019).

3.1.2 Teleconnection index

In this study, four teleconnection indices were applied: the East Central Tropical Pacific SST (El Niño 3.4), Pacific Decadal Oscillation (PDO), and Eastern Pacific/North Pacific Oscillation Index (EP/NP) from January 1959 to December 2014 and the multivariate ENSO Index (MEI V2) from January 1979 to December 2014. The teleconnection indices were taken from the National Oceanic and Atmospheric Administration (NOAA) website (available at: https://psl.noaa.gov/data/climateindices/list/) (Qian 2012).

3.2 Methods

This study used a variety of trend analysis methods, specifically the Mann–Kendall test, Pettitt test, quantile regression, and cross wavelet analysis, to test surface runoff trends in various time series and their relationship with atmospheric circulation.

3.2.1 Mann–Kendall test

The Mann–Kendall test method was first proposed by Mann (1945) and Kendall (1955). It is a nonparametric statistical test method that is used to detect, diagnose, and predict climatic trends in variables such as precipitation and surface runoff.

Assuming that the sample size of a set of time series X is n, its order is determined by

$$S_k = \sum_{i=1}^{k} r_i, r_i = \begin{cases} +1, x_i > x_j \\ 0, x_i \le x_j \end{cases}, j = 1, 2, \cdots, i \tag{1}$$

where S_k is the cumulative number when x_i is greater than x_j.

Under the assumption that the set of time series are randomly independent, it can be defined statistically as

$$UF_k = \frac{\left[S_k E(S_k)\right]}{\sqrt{Var(S_k)}}, k = 1, 2, \cdots, n \tag{2}$$

where $UF_1 = 0$, $E(S_k)$, and $Var(S_k)$ are the mean and variance of S_k respectively, and UF_k conforms to the standard normal distribution, which is calculated according to the positive sequence $x_1, x_2, \ldots, x_n$. The formula is also used to calculate UB_k using the inverse sequence $x_n, x_{n-1}, \ldots, x_1$ of the sample X.

When UF_k is greater than 0, it indicates that the original sequence is on an upward trend. When UF_k is less than 0, the original sequence is on a downward trend. If UF_k exceeds a given confidence level, the sequence is deemed to have a significant upward or downward trend. If curve UB and curve UF intersect within the confidence interval, then the time at which intersection occurs is the time when a sudden change in trend begins.

3.2.2 Pettitt test

The Pettitt test, also a nonparametric test, was originally proposed by Pettitt (1979). It can accurately find the location of a mutation and indicate its significance.

Assuming that the sample size of a set of surface runoff sequences $x_1, x_2, \ldots, x_n$ is n and that its order is $r_1, r_2, \ldots, r_n$, then the statistics is determined as

$$S_k = 2\sum_{i=1}^{k} r_i - k(n+1), k = 1, \ldots, n (j = 1, \cdots, i) \tag{3}$$

where S_k is the test result, and E is the time point at which the mutation occurred. A sudden change at a certain point in time is indicated by $S_E = 1 \le k \le n \left|S_k\right|$

$$S_E = \max_{1 \le k \le n} \left|S_k\right| \tag{4}$$

3.2.3 Quantile regression

Quantile regression was proposed by Koenker and Bassett (1978). It is a regression fitting method that quantitatively analyzes the linear relationship between independent variable X and dependent variable Y. Estimating the regression relationship between variables X and Y at different quantile levels provides a more comprehensive understanding of the global conditional distribution of variable Y. The quantile regression method has an advantage over least squares estimation because the latter only reflects the average level of the variable, which causes a certain amount of information loss. The regression coefficient values at different quantile levels are closely related to the degree of fit between variables X and Y, expressed mathematically as

$$\mathrm{T} = \mathrm{P}(y \le y(\tau)) = F(y(\tau)) \tag{5}$$

where y is a continuous random variable and τ is the probability of its i quantile $y(\tau)$. In the study of climatic time series trends, especially trends of hydrological elements, the change characteristics near the end of the distribution are particularly important. This could be significant in studying the development trend of surface runoff. Thus, several representative high quantiles of 0.75, 0.85, and 0.95 and low quantiles of 0.05, 0.15, and 0.25 were used to analyze the evolution of surface runoff in different monthly time series.

3.2.4 Cross wavelet analysis

In this study, the cross wavelet transform (XWT) and wavelet coherence (WTC) were used to analyze the characteristics of the coupling relationship between the changes in surface runoff in the MYRB and the four teleconnection indices representing atmospheric circulation. XWT was used to focus on correlations between the time series surface runoff and teleconnection indices in the high-energy area of the time and frequency scales in the study area, whereas WTC was mainly used to analyze the correlation between the time series surface runoff and teleconnection indices in low-energy areas. Assuming that the functions constructed by two time series samples are *f(t)* and *g(t)*, the definition of the cross wavelet spectrum (Hudgins and Huang 1996) is

$$C_{f \bullet g}(s) = \int \overline{W_f(s,\tau)} W_g(s,\tau) d\tau \tag{6}$$

where $\left(\overline{W_f(s,\tau)} W_g(s,\tau)\right)$ is the time scale decomposition of the two time series functions *f(t)* and *g(t)*.

The significance level of XWT comes from the square root of the product of two X^2distributed wavelet spectra (Torrence and Compo 1998). Cross wavelet analysis can effectively analyze the correlation between different signals and quantitatively represent the phase change of the signal on the time and frequency scale. In Fig. 10, the black thin solid line is the wavelet boundary effect influence cone, and the arrow within the thick black line has passed the noise test with a significance level of 0.05. The direction of the arrow indicates the phase relationship between the two. An arrow to the right indicates that the two series are in the same phase, that is, there is a certain intensity of positive correlation. An arrow to the left indicates that the two series are in reverse phase; that is, there is a certain intensity of negative correlation.

4 Results

4.1 Analysis of surface runoff trend in the MYRB

The Mann–Kendall test was used to analyze the monthly time series of surface runoff in the MYRB from 1902 to 2014, as shown in Fig. 2. The surface runoff series in January, February, and March abruptly changed around 1980 and showed a significant downward trend around 1930 (Fig. 2a–c). The difference was that the surface runoff in January showed a significant upward trend ($P < 0.05$) around 1920, whereas the time series surface runoff in February and March showed a significant upward trend ($\mathrm{P} < 0.05$) around 2010. Moreover, the surface runoff curves in both February and March intersected many times during 1960–2000 (Fig. 2b–c), indicating that the surface runoff trends of the 2 months changed drastically. Although the curves in April and May intersected at around 1915 and 2000, indicating that the trends in April and May around these two years changed, these changes were not significant (Fig. 2d–e). The difference was that the surface runoff in April had a significant downward trend during 1920–1940 and changed drastically in 1950, whereas the surface runoff in May had a significant upward trend around 1950. The trend of surface runoff in June was exceptional (Fig. 2f), with drastic changes from 1902 to 2014 and a significant upward trend ($\mathrm{P} < 0.05$) in 2010. The common feature of the time series surface runoff from July to December was that all months showed a significant upward trend ($\mathrm{P} < 0.05$) around 2010 (Fig. 2g–l). Although July had a significant upward trend ($\mathrm{P} < 0.05$) during 1920–1960, the surface runoff in July and August changed drastically from 1990 to 2010, and the surface runoff in September increased significantly ($P < 0.05$) from 1985 to 2014 (Fig. 2g–i). The surface runoff curves in October and November also changed substantially and intersected many times from 1960 to 2000 (Fig. 2j–l). The surface runoff trend in the December time series was relatively gentle, with little change.

The Mann–Kendall test results on the seasonal and annual time series surface runoff in the MYRB are shown in Fig. 3.

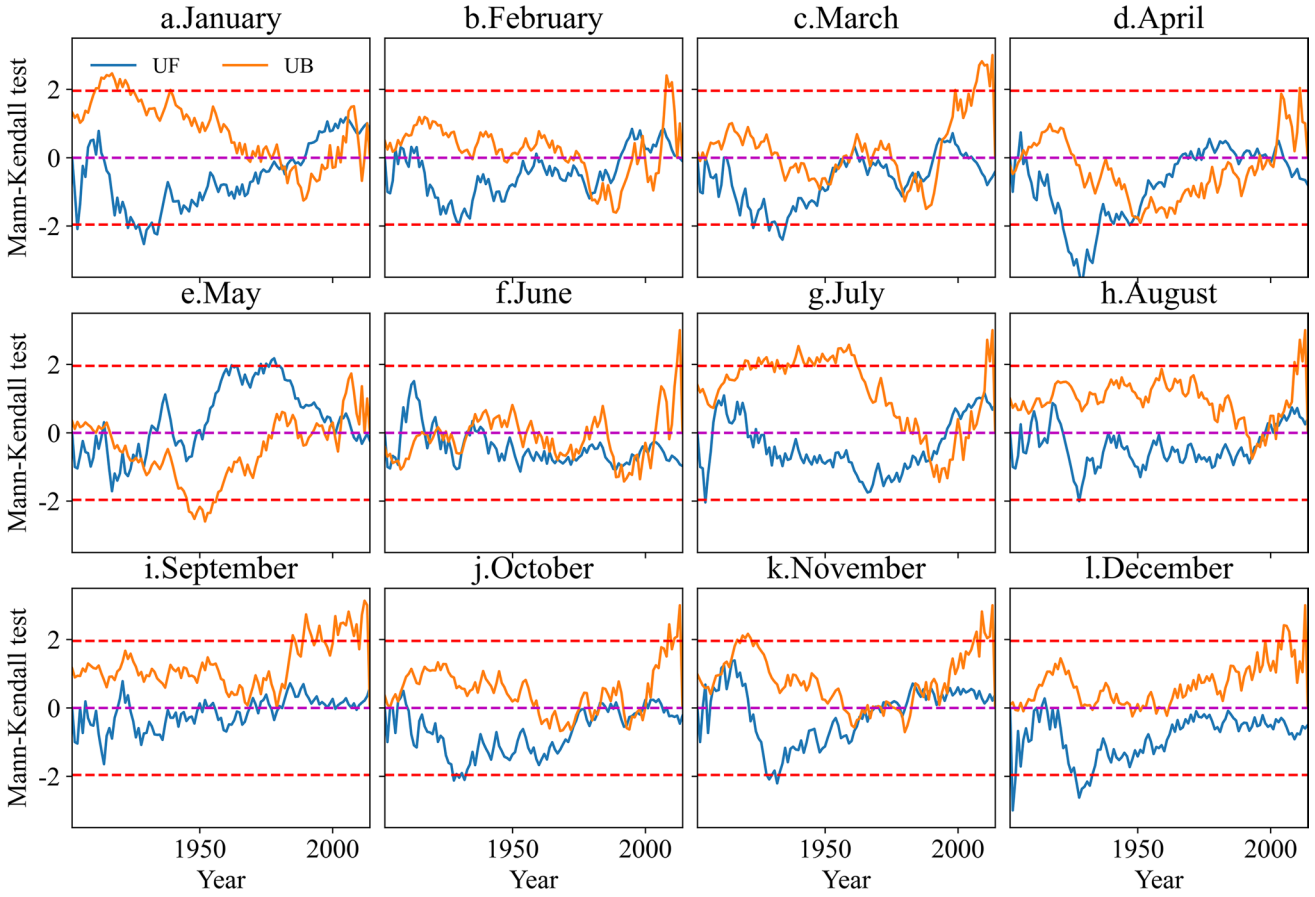

Fig. 2 Mann–Kendall test chart of monthly series runoff in the MYRB (**a–l** represent the Mann–Kendall test results from January to December, respectively)

An important feature is that the surface runoff of the four seasons as well as the annual surface runoff all showed a significant upward trend ($P < 0.05$) around 2010. The difference was that the spring, winter, and annual time series had significant downward trends ($P < 0.05$) around 1930 (Fig. 3a,d,e). There were also two substantial changes in spring and summer from 1902 to 2014 (Fig. 3a–b). The trends of surface runoff in autumn and winter changed greatly from 1975 to 2000, whereas the annual surface runoff changed strongly from 1987 to 2000 (Fig. 3c–e). In general, there were significant changes in the trends of both seasonal and annual surface runoff series from 1902 to 2014 in the MYRB.

4.2 Analysis of abrupt changes of surface runoff trend in the MYRB

Figure 4 displays the results of the Pettitt test for surface runoff in different months in the MYRB. Except for February, March, May, and July, changes occurred relatively early in the MYRB, with abrupt changes in most subareas before 1950 (Figs. 4a,d,f,h–l). A small number of subareas had abrupt changes around 1980. Among these, the earliest was the abrupt change in overall regional surface runoff in September, although only a small part of the northwest and central areas had an abrupt change around 1998 (Fig. 4i). The surface runoff in October changed significantly ($P < 0.05$) around 1966 in most parts of the northeast. In contrast, abrupt changes in the time series surface runoff of February, March, May, and July occurred in later years; some areas changed around 2014 (Fig. 4b,c,e,g). For the February time series surface runoff, only the central region changed around 1920, whereas most of the northern and southern regions changed abruptly around 1985 (Fig. 4b). There were no overall changes in the time series surface runoff trends in February in the MYRB from 1902 to 2014. Compared with surface runoff in other months, surface runoff in March most changed abruptly in about 2014, mainly in the northern and central regions (Fig. 4c). The southern region had a significant abrupt surface runoff change in 1990. The distribution of abrupt changes in the surface runoff sequence in May differed significantly from north to south (Fig. 4e). The surface runoff to the north of the central area changed abruptly around 1940, but the surface runoff in the south changed abruptly after 1998. It is evident in

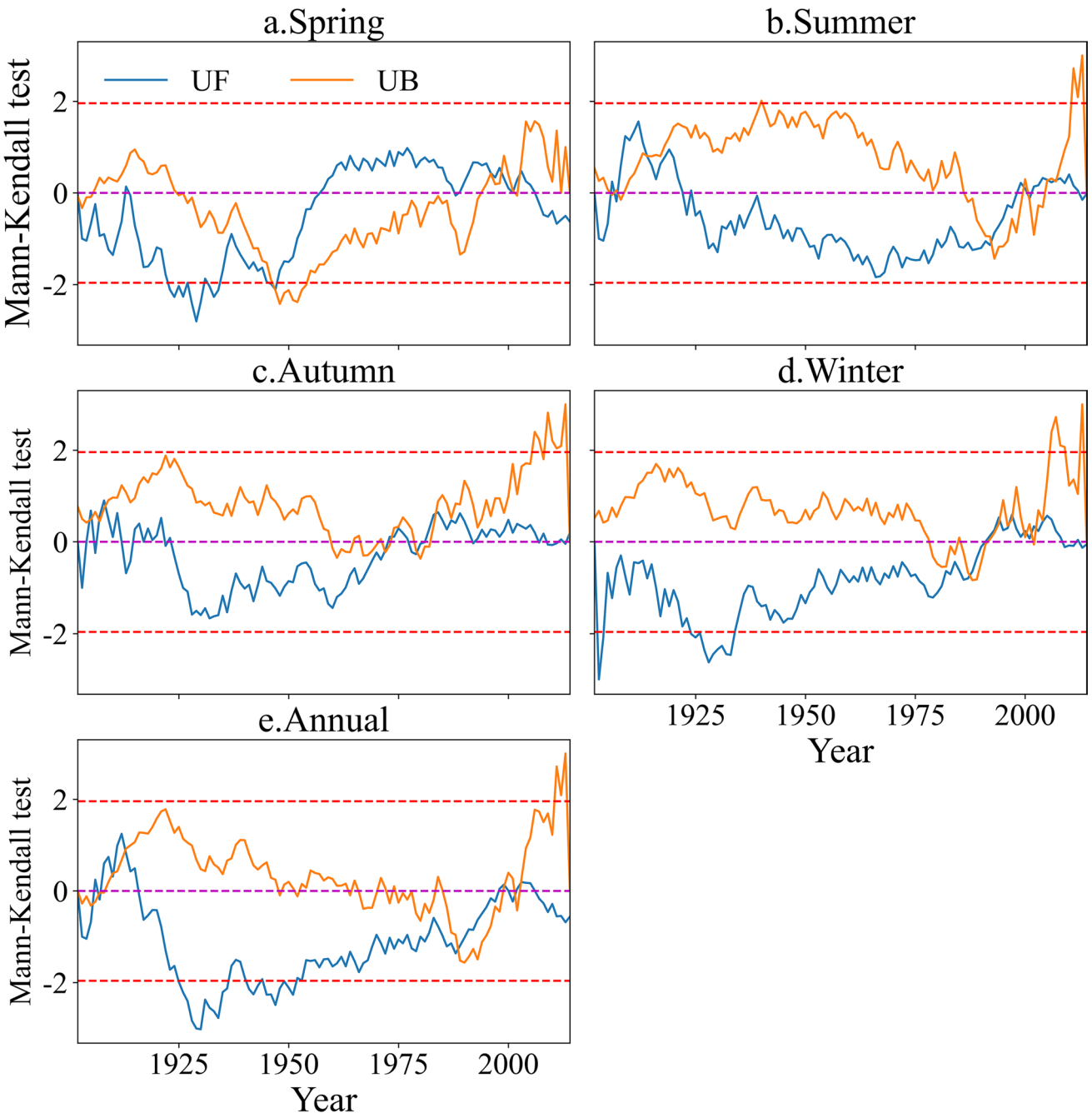

Fig. 3 Mann–Kendall test chart of seasonal and annual runoff in the MYRB (**a**–**e** represent the Mann–Kendall test results from Spring to Winter and Annual, respectively)

the monthly data that most of the northwestern and southwestern regions changed abruptly ($P < 0.05$). In July, most areas changed abruptly around 1990, but a small number of areas in the north and southeast changed around 1965. The northwest surface runoff sequence shows a significant abrupt change in 1990. In general, the distribution of years of abrupt surface runoff change in each monthly time series in the MYRB was different. In addition, the degrees the significance of the abrupt changes in surface runoff in different time series in the MYRB were also different.

Figure 5 represents the distribution of mutations among the surface runoff years in each seasonal and annual sequence in the MYRB. The results show that the distributions of spring and summer surface runoff mutation years were relatively consistent and that the changes all occurred around 1940 (Fig. 5a,b). In the seasonal and annual time

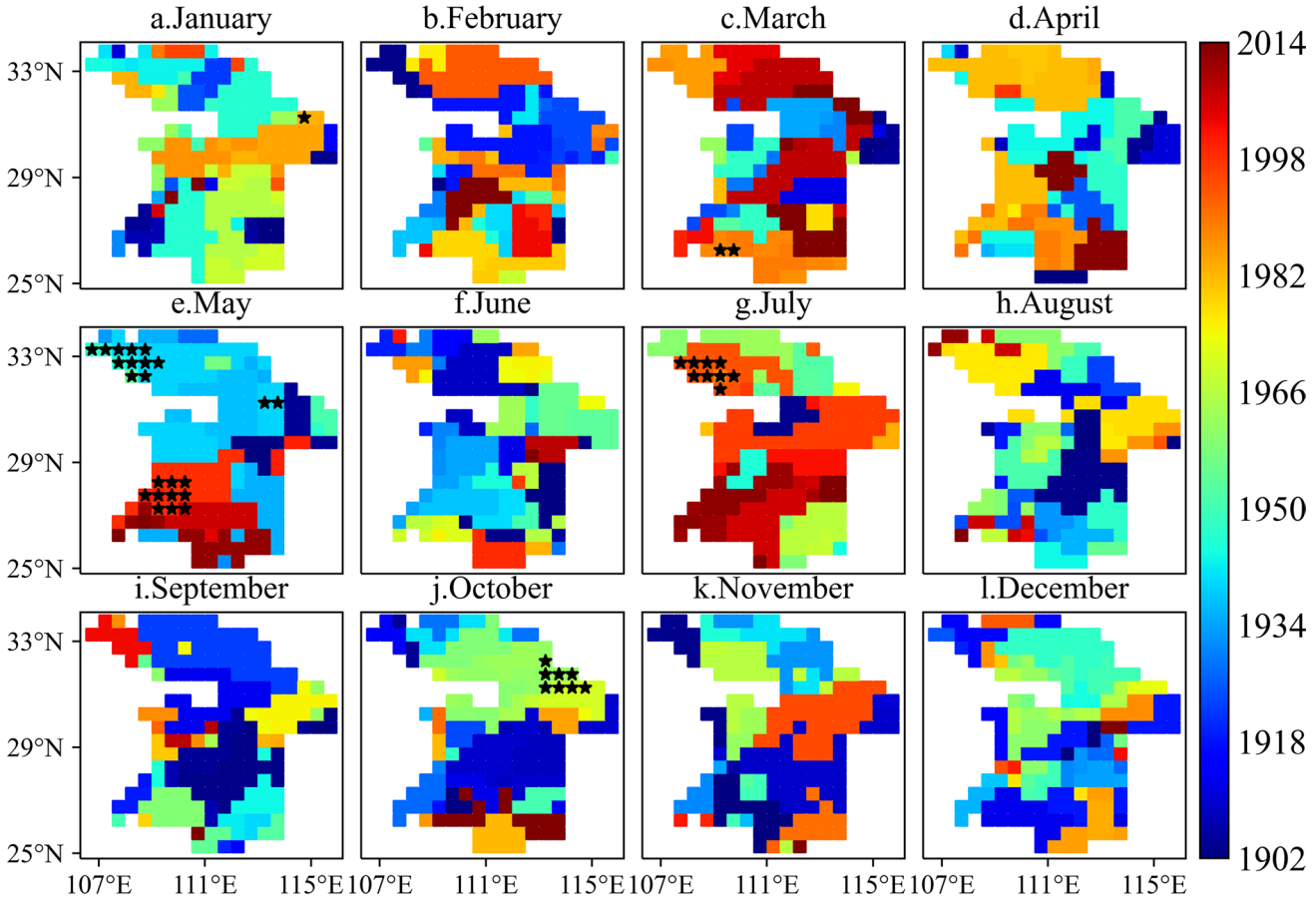

Fig. 4 Distribution of abrupt changes in monthly runoff in the MYRB (The significance test was performed, and the grids that reached the significance level were distinguished by "*")

series surface runoff mutation year distribution map, only the mutations in the spring and summer surface runoff series reached the level of significance. Abrupt changes in the autumn, winter, and annual series occurred relatively early (Fig. 5b,d,e). Only a few grids in the MYRB, in each month, reached the significance level ($P < 0.05$), indicating that while surface runoff in the MYRB changed from 1902 to 2014, only a few regions had significant changes.

4.3 Quantile regression analysis of surface runoff series in the MYRB

Figure 6 shows the quantile regression results for surface runoff time series of different months. Except for January, February, and May, the fitted time series surface runoff trends at the high quantiles of 0.85 and 0.95 were quite different (Figs. 6c,d,f–l). Surface runoff in March, April, June, and July changed slowly at the 0.95 quantile level, whereas the absolute values of the slopes of the straight lines at the 0.75 and 0.85 quantile levels were large and negative and the trends were obvious (Fig. 6c,d,f,g). The absolute values of the linear slopes of the surface runoff in June, September, October, and November at the 0.95 quantile level were large and negative, whereas the changes were gentle at the 0.75 and 0.85 quantile levels (Figs. 6f,h–j). The analysis above indicates that over time, climate change has had a certain degree of impact on surface runoff at high quantiles levels. However, at low quantile levels, except for June, trends in months were not obvious. The overall quantile distribution in June showed a convergent pattern, and the changing trend of the low quantile level was opposite that of the high quantile level, which indicated that climate change had a particularly obvious impact on surface runoff in June time series (Fig. 6f). No obvious trend change was observed via least squares fitting over the 12 months, indicating that climate change had little effect on average surface runoff. At the later stages of the distribution, the monthly quantile regression results were not significant, but there were certain changes in the fitted trend.

The results of further analysis of the slopes of the quantile regressions of different months are shown in Fig. 7. Except for May, June, September, and November,

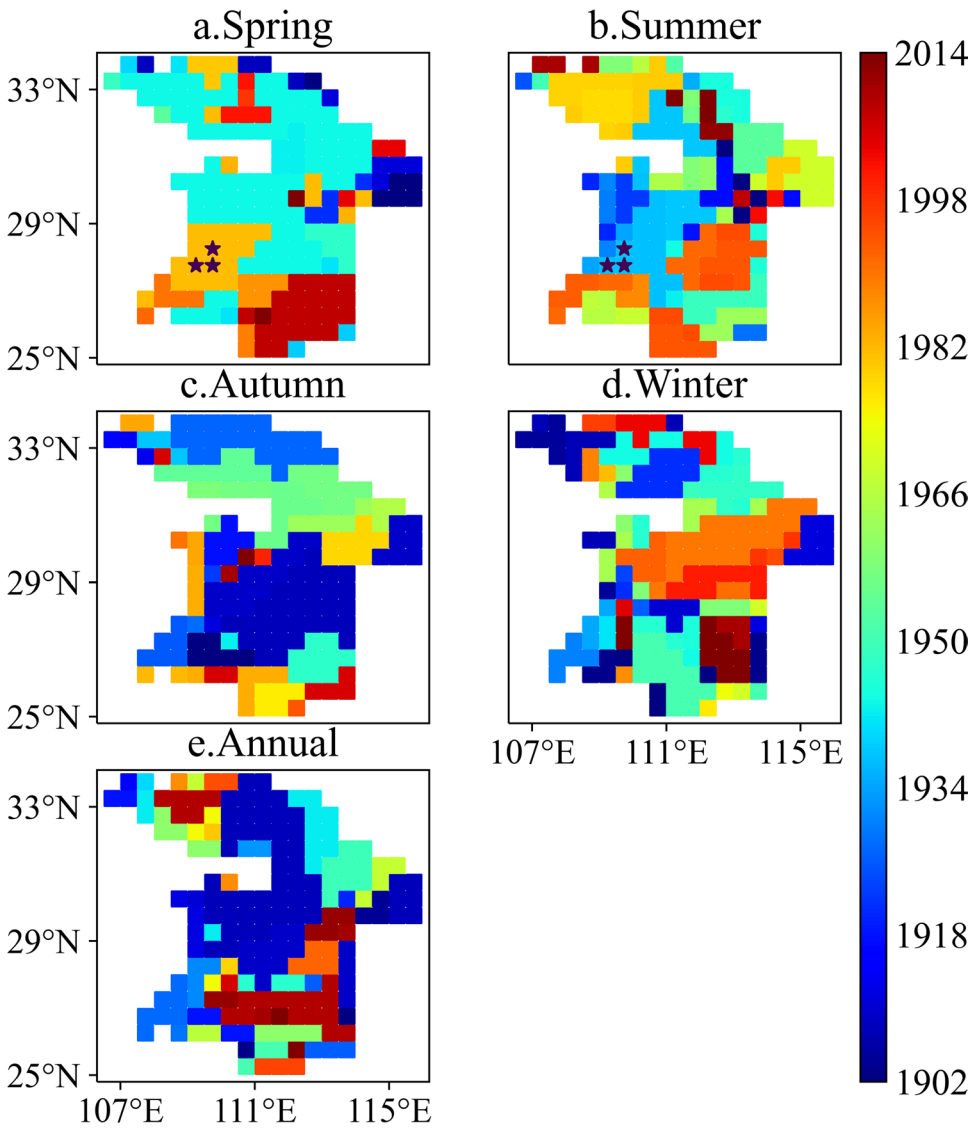

Fig. 5 Distribution map of seasonal and annual runoff abrupt changes in the MYRB (the significance test was performed, and the grids that reached the significance level were distinguished by "*")

a significant feature was that the slopes of the quantile regression estimates of surface runoff fluctuated within the significance interval of the least squares regression (Figs. 7a–d,g,i,k). This showed that the impact of climate change on surface runoff was relatively constant throughout the distribution in most monthly time series. The quantile regression slopes in May, June, September, and November had larger changes than in other months, at the tails of the distributions (Figs. 7e–f,i,k). The impact of surface runoff at the high and low quantile levels was greater than the impact at median quantile levels. From January to December, the slopes of the regression estimates for each quantile were relatively small, and the changes were mainly concentrated at the tails of the distributions (i.e., the high quantiles and low quantiles), which is consistent with the results obtained in Sects. 4.1 and 4.2.

Figure 8 shows the quantile regression results for surface runoff in the seasonal and annual time series. Spring had a significant upward trend at the 0.05 and 0.95 quantile regression levels (Fig. 8a), summer had a greater upward trend at the 0.95 quantile regression level (Fig. 8b), autumn had an obvious downward trend at the 0.95 quantile regression level (Fig. 8c), and winter had a clear upward trend at the 0.85 quantile regression level (Fig. 8d). The annual surface runoff series had some downward trend in the 0.85 quantile level regression, but there was a clear upward trend at the 0.95 quantile level (Fig. 8e). The analysis verified that climate change had a greater impact on the tail end of the time series surface runoff. Generally, no obvious surface runoff trends were obtained by least square regression The curves tended to be horizontal, and the fitting was poor. However, the quantile regression of seasonal and annual surface runoff showed

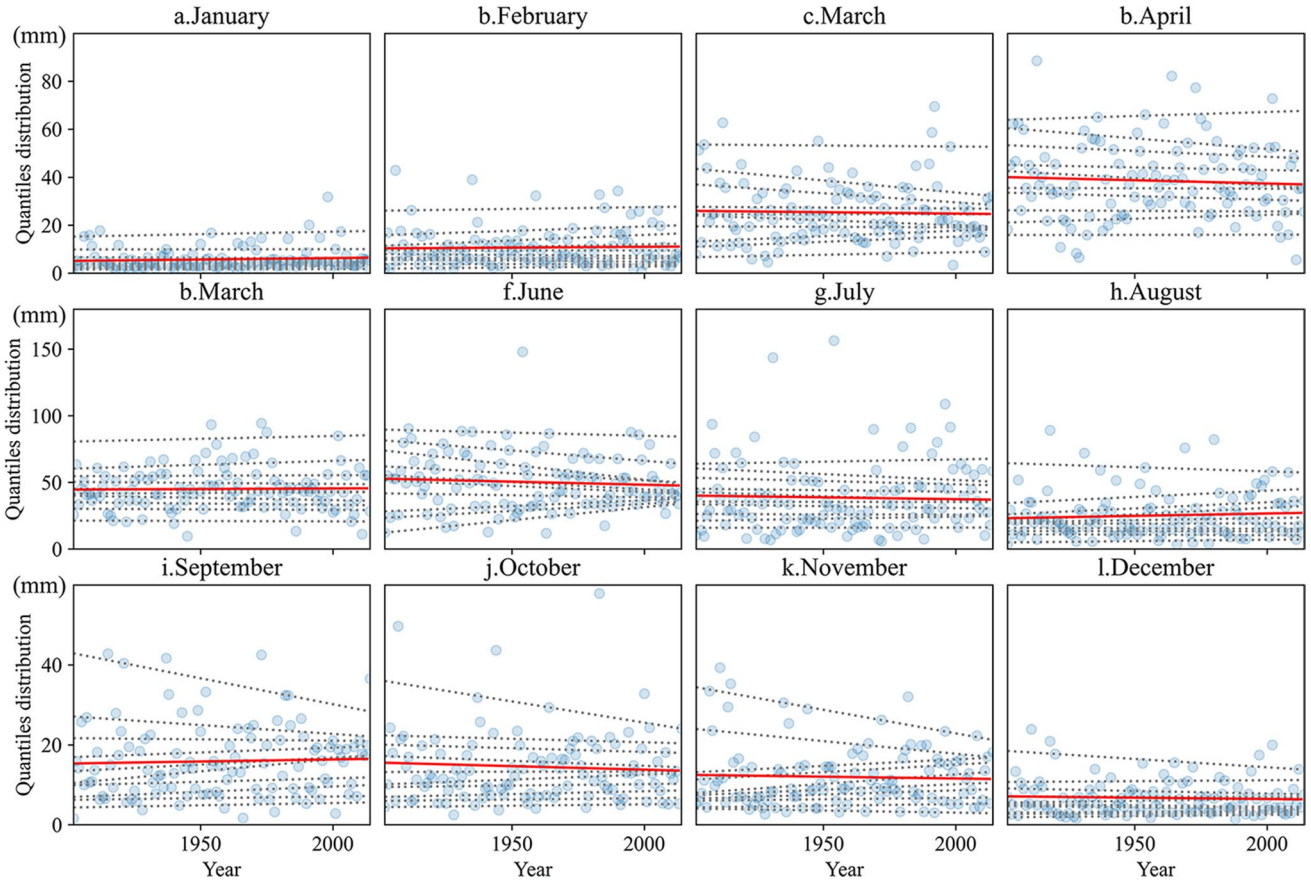

Fig. 6 Quantile regression distribution of monthly runoff series in the MYRB (the red solid line in the figure was the result of least squares fitting, the gray dashed line was the regression result of different quantiles, from bottom to top were 0.05, 0.15, 0.25, 0.35, 0.45, 0.55, 0.65, 0.75, 0.85, and 0.95 quantile regression fitting results)

that different quantile levels had different trends. Although the regression fitting results of each season and the annual quantile analysis did not reach the level of significance, the distribution of quantile values in the different seasons still reflected certain changes in surface runoff trend.

The slope distribution of the seasonal and annual surface runoff quantile regressions is shown in Fig. 9. The regression trends of spring, summer, and winter surface runoff at the middle and low quantile levels are not obvious, with their slopes fluctuating around 0 (Fig. 9a,b,d). The surface runoff results in the spring, summer, and annual time series have larger and positive slopes at the high quantile level (Fig. 9a,b,e). The regression trends for the middle and low quantile levels of the autumn time series are not obvious, but they are different from those other seasons in that the absolute value of the slope is larger and negative at the high quantile level (Fig. 9c), indicating that the high quantile autumn surface runoff has been decreasing over time. This is consistent with the analytical conclusions obtained through Fig. 8, which showed that climate had a greater influence on seasonal and annual time series surface runoff at high quantile levels. The quantile regression analysis of the time series surface runoff, at different quantile levels, provides a more comprehensive and accurate understanding of surface runoff trends in the MYRB and the impact of climate change on those trends.

4.4 Analysis of teleconnection between surface runoff and atmospheric circulation in the MYRB

XWT and WTC were used to study the coupling relationship between regional surface runoff and atmospheric circulation. Figure 10 shows the results of the application of XWT and WTC the surface time series surface runoff and four representative teleconnection indices in the middle and lower reaches of the Yangtze River. It can be seen from Fig. 10 that the distribution of the high-energy region of XWT is roughly the same as the distribution of the WTC low-energy region. Among the indices, El Niño 3.4, PDO and EP/NP from January 1950 to December 2014 have a higher agreement with the time series surface runoff in the XWT high-energy region and the WTC low-energy region (Figs. 10a–c,

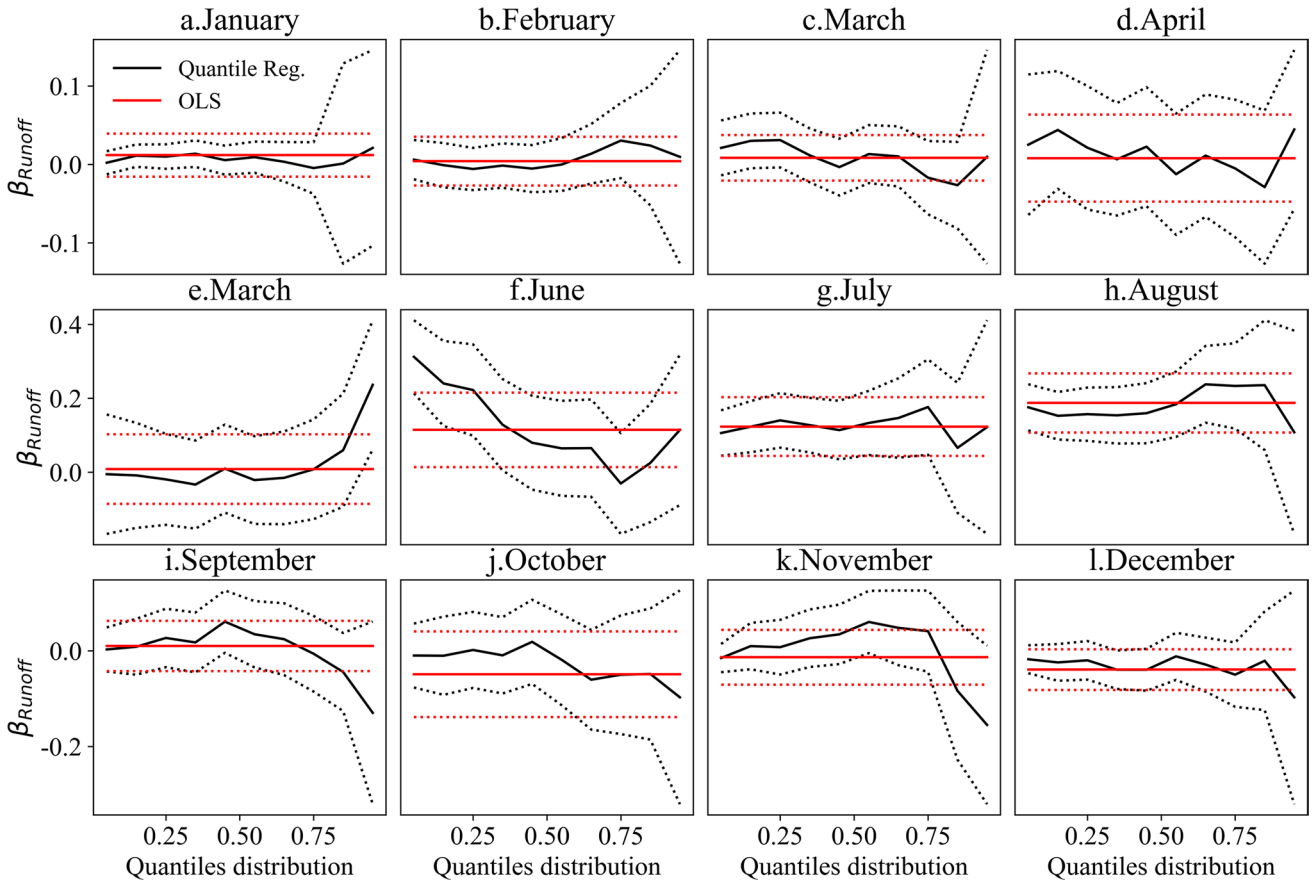

Fig. 7 Distribution of quantile regression slopes of monthly runoff series (the black solid lines in the figure were the slope corresponding to the 10 quantile regression estimates used in this study. The black dashed line was the 95% significance interval corresponding to the slope of the quantile regression estimate, the red solid line was the slope of the least squares regression estimate, and the red dashed line was its significance interval)

e–g). Meanwhile, the phase relationship between time series surface runoff and teleconnection indices can be determined using the directional arrows of the cross wavelet transform and wavelet coherence. In the XWT analysis of surface runoff and El Niño 3.4, the results show high-energy areas with arrows mainly pointing to the right, indicating that the two series at 1–2 a (1950s–1975s), 1–2 a (1990s), and 1–2 a (2010s–2014s) had a significant and strong positive correlation (Fig. 10a). In the WTC results, the low-energy region also has arrows pointing to the right, indicating a significant positive correlation ($P < 0.05$) between the two sequences at 1–2 a (1960s–1970s) (Fig. 10e). In the analysis of surface runoff and PDO, the XWT results indicate the same change periods as in the first XWT result, but the distribution years are different (Fig. 10b). In the WTC results, the low-energy zone is more dispersed (Fig. 10f). In the analysis of surface runoff and EP/NP, the XWT results show that the high-energy area has mainly leftward-directed arrows, indicating a significant negative correlation ($P < 0.05$) at 1–2a (1950s–1960s) and 1–2a (1970s–1980s and 2000s) between the two sequences (Fig. 10c). The low-energy area also showed a significant negative correlation ($P < 0.05$) (Fig. 10g). There was a strong positive phase correlation between the time series surface runoff and MEI V2 from January 1979 to December 2014, but the periodic changes were longer, mainly at 1–4a (1980s), 2–3a (1985s–1990s), 1–4a (1990s–2000s), and 1–4a (2010s) (Fig. 10d). In general, a strong correlation exists between the various climatic teleconnection indices and time series surface runoff in this region, indicating a significant coupling relationship ($P < 0.05$) between atmospheric circulation and surface runoff in the MYRB.

5 Discussion

5.1 Data availability

A limitation of this study was that the data came from machine learning simulations, rather than actual observation

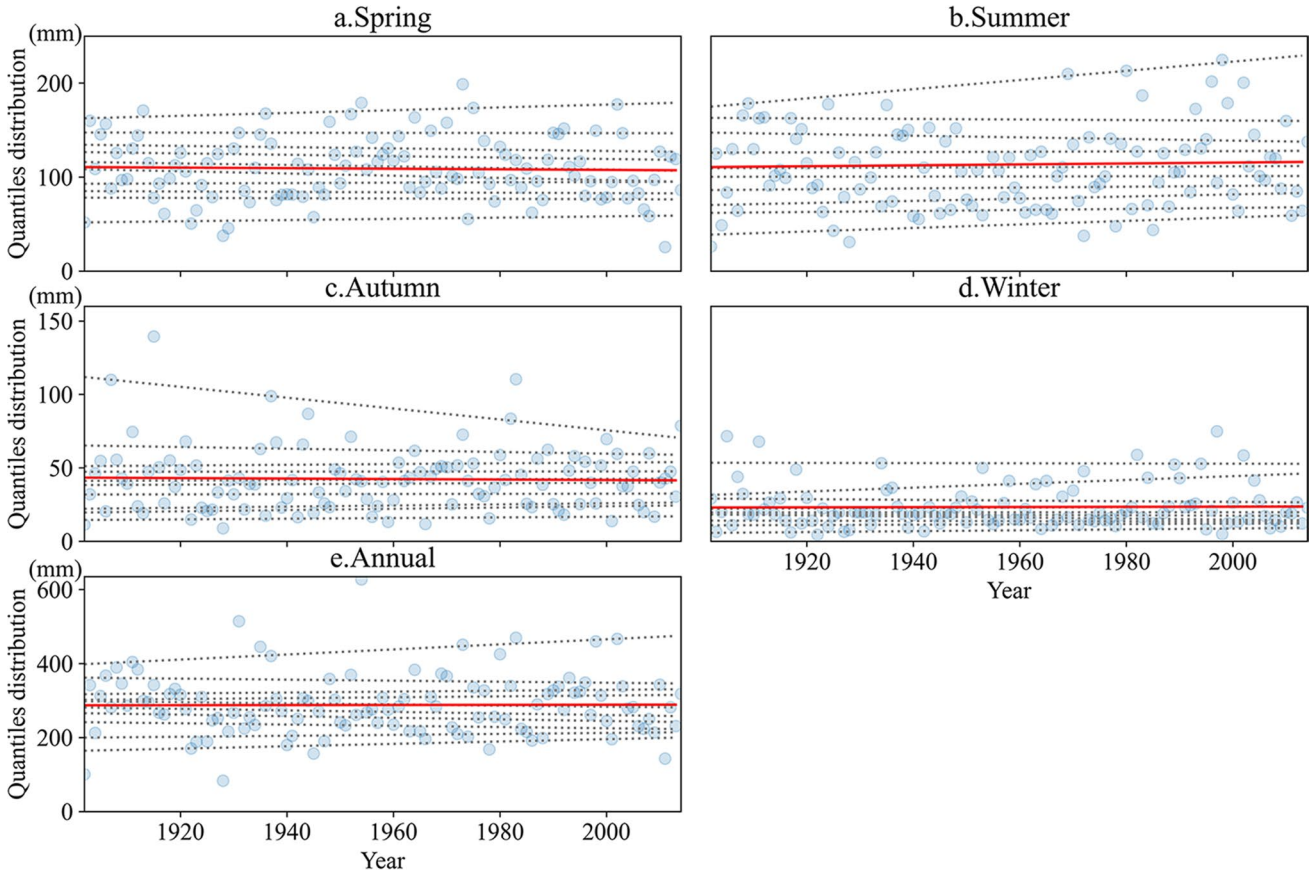

Fig. 8 Quantile regression distribution of seasonal and annual runoff series in the MYRB (the red solid line in the figure was the result of least squares fitting, the gray dashed line was the regression result of different quantiles, from bottom to top were 0.05, 0.15, 0.25, 0.35, 0.45, 0.55, 0.65, 0.75, 0.85, and 0.95 quantile regression fitting results)

data, and these may be different from real surface runoff conditions. However, the sample data used to train the machine learning model, and hence, the related factor data, are real observations (Do et al. 2018; Gudmundsson et al. 2017). Therefore, the data used in this study are believed to approximate true surface runoff trends and changes. In any further research, different methods may be appropriate for investigation of correlations between influencing factors and changing surface runoff.

5.2 Study methods of surface runoff changes in the MYRB

This study used a variety of methods to test time series data trends (Mann–Kendall test, Pettitt test, and quantile regression) allowing the trend results to be verified mutually. The Mann–Kendall test is a classic trend test method and has been widely used with long-term climatic series (Mann 1945; Kendall 1955). To understand the changes in surface runoff in the MYRB from 1902 to 2014, the Pettitt test was applied to the gridded data to identify abrupt changes (Pettitt 1979). Trend analyses of the various time series surface runoff results in the MYRB improved understanding of the surface runoff characteristics and the change laws of the study area, whereas quantile regression assessed the surface runoff trends over different quantiles (Koenker and Bassett 1978). Assessing the changes of surface runoff under different quantiles allows a more comprehensive understanding of the surface runoff information. This removes the deficiency of analyzing surface runoff evolution by using only mean values and also avoids the influence of outliers on the overall trends (Benoit and Van den Poel 2009). The combined use of these methods on different aspects of the surface runoff trends in the MYRB makes these results richer and more credible than those of previous studies using individual methods.

5.3 Practical significance of surface runoff changes in the MYRB

From ancient times to the present, human activities have greatly changed the human–land relationship in the middle

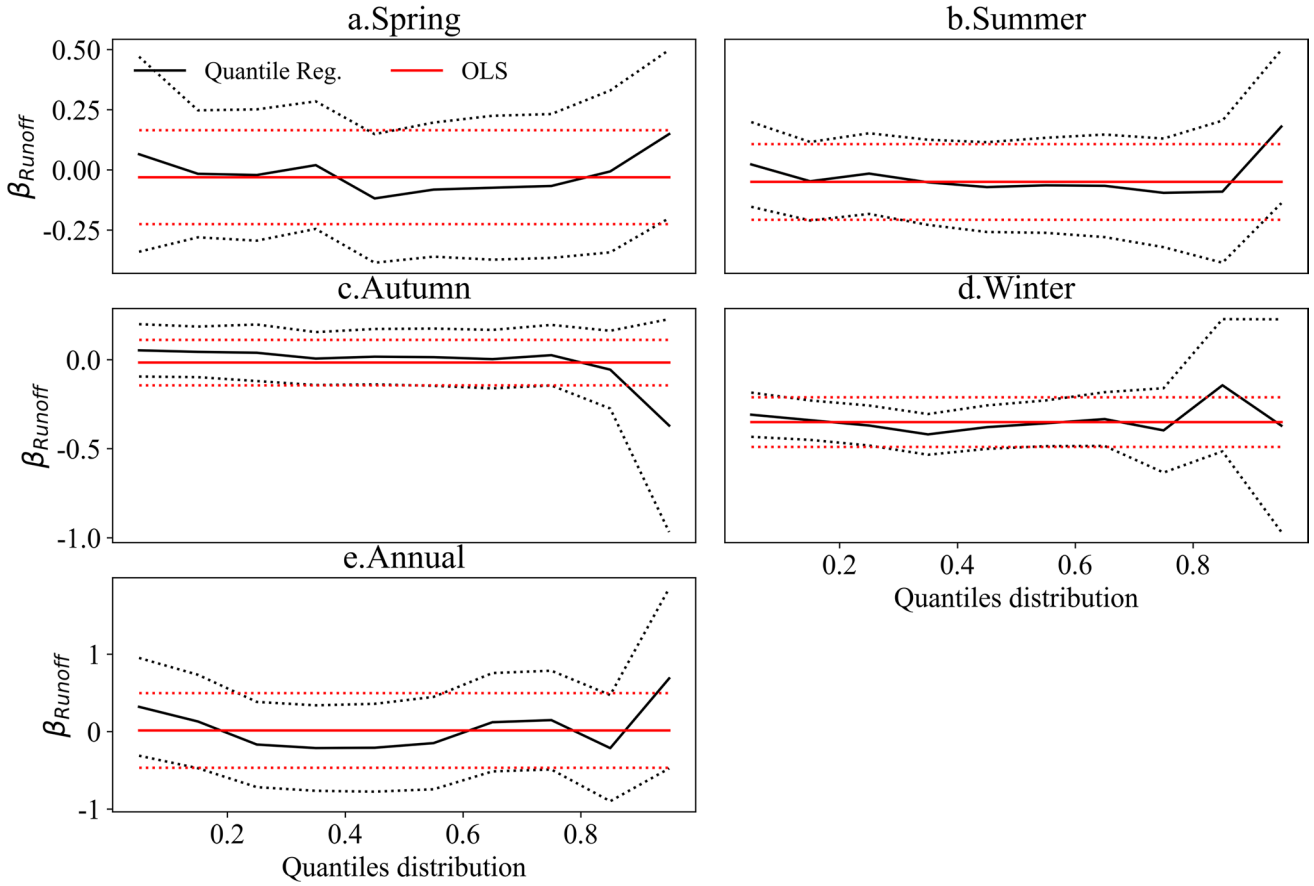

Fig. 9 Distribution of quantile regression slopes of seasonal and annual runoff series in the MYRB (the black solid lines in the figure were the slope corresponding to the 10 quantile regression estimates used in this study. The black dashed line was the 95% significance interval corresponding to the slope of the quantile regression estimate, the red solid line was the slope of the least squares regression estimate, and the red dashed line was its significance interval)

reaches of the YRB (Cui et al. 2013). While the YRB has facilitated the economic development of coastal areas, it has also brought threats to the survival of people (Huang et al. 2009). In this study, various methods were used to detect changes in surface runoff in the MYRB. The surface runoff trends of different monthly, seasonal, and annual series were found to be different (Jiang et al. 2007). This suggests that changes in climatic factors have specific impacts on surface runoff changes. Other research has found that climate change and human activities are important factors affecting surface runoff (Farsi and Mahjouri 2019). Surface runoff in the MYRB experienced a noteworthy and drastic increase in July 1998 linked to a major historical flood disaster (Zong and Chen 1998). Generally, surface runoff in the MYRB is decreasing, and this is closely related to the background of global warming (Fig. 6g, h).

5.4 Analysis of teleconnection between surface runoff in the MYRB and atmospheric circulation

This study sought a better understanding of the relationship between surface runoff trends and atmospheric circulation as reflected in teleconnection indices. A significant correlation was found between the surface runoff changes in the study area and four indices (El Niño 3.4, PDO, EP/NP, and MEI V2), indicating that atmospheric circulation has had a significant influence on surface runoff in the MYRB (Sun and Cheng 2008). Other studies found that surface runoff in the MYRB decreased both before and after the summer drought in 1980. This is also believed to have been closely related to global warming (Li et al.

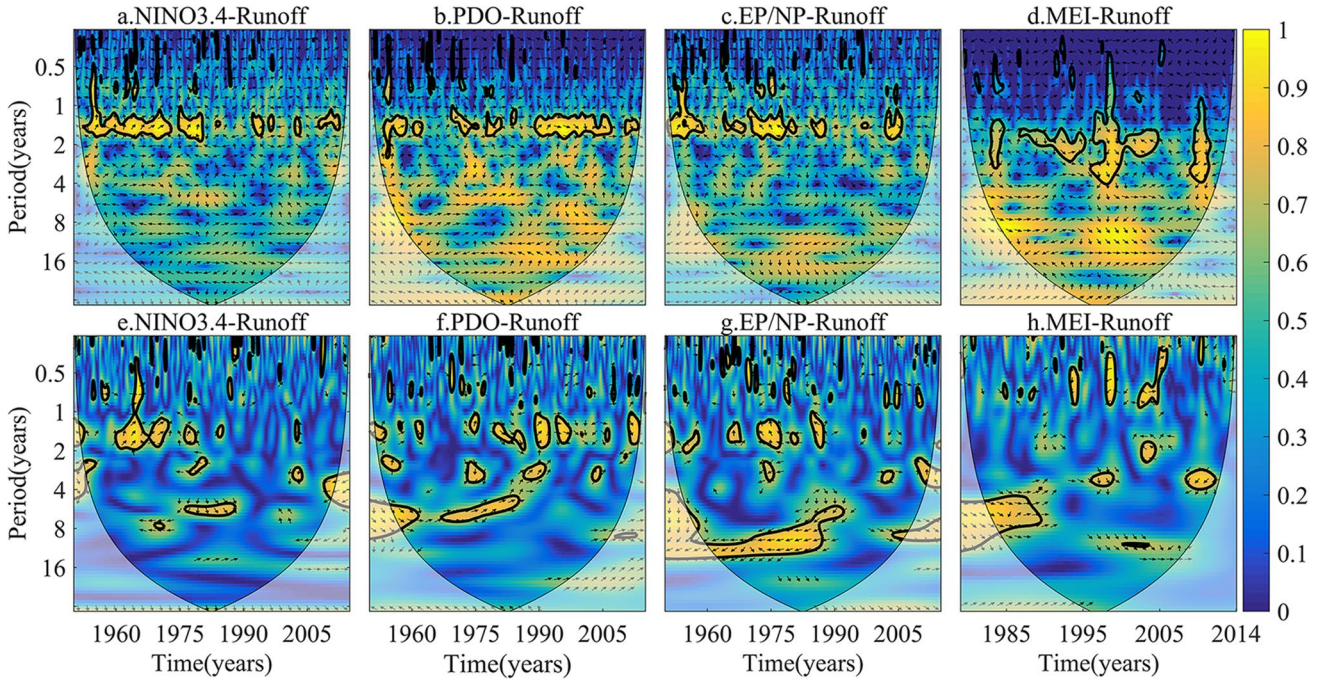

Fig. 10 The results of XWT and WTC between annual runoff in the MYRB and four representative teleconnection indexes (e.g., El Niño 3.4, PDO, EP/NP, and MEI V2), respectively

2016). Of the indexes, the PDO is the most significantly related to surface runoff trends (Fig. 10b,f).

6 Conclusion

This study adopted the quantile regression method and the cross wavelet method, which have been widely used in many fields. Relationships between the change of surface runoff in the MYRB and four teleconnection indices were studied from different aspects, and the results were relatively rich and comprehensive. The specific conclusions were as follows:

(1) The trends in surface runoff annual series from 1902 to 2014 in the MYRB have changed significantly. The longest and most significant upward trend occurred from 1987 to 2000. Spring, winter, and the annual data showed significant downward trends ($P < 0.05$) around 1930.

(2) The annual series surface runoff mutation years varied across the MYRB (e.g., surface runoff in the central region changed abruptly around 1918, whereas surface runoff in the northern and southern regions changed abruptly around 2000). The mutation years of adjacent regions were more consistent, reflecting continuities across the underlying surface. There was also a degree of correlation between surface runoff changes and the distribution of water systems

(3) A significant correlation ($P < 0.05$) exists between time series surface runoff in the MYRB and the four representative teleconnection indices of atmospheric circulation (El Niño 3.4, PDO, EP/NP, and MEI V2).

Acknowledgements Runoff dataset were derived from https://www.research-collection.ethz.ch/handle/20.500.11850/324386?show=full, (Do et al. 2018; Gudmundsson et al. 2018b; Kim et al., 2017), while the four teleconnection indexes (e.g., El Niño 3.4, PDO, EP/NP, and MEI V2) were mainly from the National Oceanic and Atmospheric Administration (NOAA) website (available at: https://psl.noaa.gov/data/climateindices/list/) (Qian et al.,2012). We would like to express our sincere thanks to all data supporters and websites. Meanwhile, the research is supported by Visiting Researcher Fund Program of State Key Laboratory of Water Resources and Hydropower Engineering Science (2020SWG01) and Youth Fund for Humanities and Social Science Research of the Ministry of Education (No. 20YJCZH207).

Author contribution Wenyu Wang analyzed the coupling relationship between the change of surface runoff in the middle reaches of the Yangtze River and the atmospheric teleconnection index, and was the main contributor to the manuscript. Peng Yang provided ideas and theoretical guidance. Jun Xia revised the thought and direction of the thesis. Shengqing Zhang collected datasets and related materials. Wei Cai collected datasets and related materials. All authors read and approved the final manuscript.

Funding Visiting Researcher Fund Program of State Key Laboratory of Water Resources and Hydropower Engineering Science (2020SWG01).

Data availability The datasets generated during the current study are available in the https://www.research-collection.ethz.ch/handle/20.500.11850/324386?show=full and https://psl.noaa.gov/data/climateindices/list.

Code availability Not applicable.

Declarations

Ethics approval Not applicable.

Consent to participate Not applicable.

Consent for publication Not applicable.

Conflict of interest The authors declare no competing interests.

References

Benoit DF, Van den Poel D (2009) Benefits of quantile regression for the analysis of customer lifetime value in a contractual setting: an application in financial services. Expert Syst Appl 36:10475–10484

Chen J (2020) Integrated management of the Yangtze River Basin. Evolution and Water Resources Utilization of the Yangtze River. Springer, Singapore, pp 385–459

Chai Y et al (2019) Influence of Climate variability and reservoir operation on streamflow in the Yangtze River. Sci Rep 9:5060

Chen F et al (2019) Major advances in studies of the physical geography and living environment of China during the past 70 years and future prospects. Sci China Earth Sci 62:1665–1701

Chen W, Chi G, Li J (2020) Ecosystem services and their driving forces in the Middle Reaches of the Yangtze River Urban Agglomerations, China. Int J Environ Res Public Health 17(10):3717

Cui L et al (2013) Dynamics of the lakes in the middle and lower reaches of the Yangtze River basin, China, since late nineteenth century. Environ Monit Assess 185:4005–4018

Ding T, Gao J, Tian S et al (2014) Chemical and isotopic characteristics of the water and suspended particulate materials in the Yangtze River and Their Geological and Environmental Implications. Acta Geol Sin 01:276–360

Do HX, Gudmundsson L, Leonard M, Westra S (2018) The Global Streamflow Indices and Metadata Archive (GSIM) – Part 1: the production of a daily streamflow archive and metadata. Earth System Science Data 10:765–785

Farsi N, Mahjouri N (2019) Evaluating the contribution of the climate change and human activities to runoff change under uncertainty. J Hydrol 574:872–891

Ghiggi G, Humphrey V, Seneviratne SI et al (2019) GRUN: an observation-based global gridded runoff dataset from 1902 to 2014. Earth Syst Sci Data 11(4):1655–1674

Grinsted A. Moore J C. Jevrejeva S (2004) Application of the cross wavelet transform and wavelet coherence to geophysical time series. Nonlinear Process Geophys 11,5/6(2004-11-18), 11(5/6):561–566

Gudmundsson L, Hồng ĐX, Leonard M, Westra S, Seneviratne SI (2017) The Global Streamflow Indices and Metadata Archive (GSIM) – Part 2: quality control, time-series indices and homogeneity assessment. Earth System Science Data 10:1–27

Huang J, Wu Y, Qin C et al (2009) Research on the human-water relationship in the middle Reaches of Yangtze River. International Conference on Environmental Science & Information Application Technology. IEEE

Hudgins L, Huang J (1996) Bivariate wavelet analysis of Asia monsoon and ENSO. Adv Atmos Sci 13(3):299–312

Jiang T, Su B, Hartmann H (2007) Temporal and spatial trends of precipitation and river flow in the Yangtze River Basin, 1961–2000. Geomorphology 85:143–154

Kalisa W, Igbawua T, Ujoh F et al (2021) Spatio-temporal variability of dry and wet conditions over East Africa from 1982 to 2015 using quantile regression model. Natural Hazards 3:1–30

Kendall M G (1948) Rank correlation methods

Kim H, Oki T(2015) The pilot phase of the global soil wetness project phase 3. AGU Fall Meeting Abstracts. GC24B-05

Koenker R, Bassett Jr G (1978) Regression quantiles. Econometrica: Journal of the Econometric Society 33–50

Kuang C-P et al (2014) Multi-time scale analysis of runoff at the Yangtze estuary based on the Morlet Wavelet Transform method. J Mt Sci 11:1499–1506

Lai X, Jiang J, Yang G, Lu XX (2014) Should the Three Gorges Dam be blamed for the extremely low water levels in the middle-lower Yangtze River? Hydrol Process 28:150–160

Li S, Feng G, Hou W (2016) Summer drought patterns in the middle-lower reaches of the yangtze river basin and their connections with atmospheric circulation before and after 1980. Advances in Meteorology 2016:1–18

Li X et al (2021) Changes in precipitation extremes in the Yangtze River Basin during 1960 2019 and the association with global warming ENSO and local effects. Sci Total Environ 760:144244

Liu G (2008) On geo-basis of river regulation —A case study for the middle reaches of the Yangtze River. Sci China Ser e: Technol Sci 51:494–505

Mann HB (1945) Nonparametric test against trend. Econometrica 13:245–259

Meng Z, Zhang F, Luo D et al (2019) Review of Chinese atmospheric science research over the past 70 years: Synoptic meteorology. Sci China Earth Sci 62(12):1946–1991

Papacharalampous G, Tyralis H, Koutsoyiannis D (2018) Predictability of monthly temperature and precipitation using automatic time series forecasting methods. Acta Geophys 66:807–831

Pettitt AN (1979) A non-parametric approach to the change-point problem. J Roy Stat Soc 28:126–135

Pokhrel Y et al (2021) Global terrestrial water storage and drought severity under climate change, *Nature*. Clim Change 11:226–233

Qian WH (2012) Atmospheric teleconnections and regional-scale atmospheric anomalies over the Northern Hemisphere. chin j geophysics 55:1449–1461

Resende NC, Miranda JH, Cooke R, Chu ML, Chou SC (2019) Impacts of regional climate change on the runoff and root water uptake in corn crops in Parana, Brazil. Agric Water Manag 221:556–565

Shan L et al (2018) Characteristics of dry-wet abrupt alternation events in the middle and lower reaches of the Yangtze River Basin and the relationship with ENSO. J Geog Sci 28:1039–1058

Su B. Xiao B. Zhu D, et al. (2005) Trends in frequency of precipitation extremes in the Yangtze River basin, China: 1960–2003. Int Assoc Sci Hydrol Bull 50(3):–492

Sun Z, Huang Q, Opp C, Hennig T, Marold U (2012) Impacts and implications of major changes caused by the three gorges dam in the middle reaches of the Yangtze River, China. Water Resour Manage 26:3367–3378

Sun W, Cheng B (2008) Application of cross wavelet transformation to analysis on regional climate variations. J Appl Meteorol Clim 19(4):479–487

Torrence C, Compo GP (1998) A practical guide to wavelet analysis. Bull Am Meteor Soc 79:61–78

Trusel LD et al (2018) Nonlinear rise in Greenland runoff in response to post-industrial Arctic warming. Nature 564:104–108

Wang B et al (2013) Distribution of perfluorinated compounds in surface water from Hanjiang River in Wuhan, China. Chemosphere 93:468–473

Yang W, Jin F, Si Y, Li Z (2021) Runoff change controlled by combined effects of multiple environmental factors in a headwater catchment with cold and arid climate in northwest China. Sci Total Environ 756:143995

Ye X, Xu C-Y, Li Y, Li X, Zhang Q (2017) Change of annual extreme water levels and correlation with river discharges in the middle-lower Yangtze River: Characteristics and possible affecting factors. Chin Geogra Sci 27:325–336

Yuan W, Yin D, Finlayson B, Chen Z (2012) Assessing the potential for change in the middle Yangtze River channel following impoundment of the Three Gorges Dam. Geomorphology 147–148:27–34

Zhang Q, Gemmer M, Chen J (2008) Climate changes and flood/drought risk in the Yangtze Delta, China, during the past millennium. Quatern Int 176–177:62–69

Zhang Q, Xiao M, Singh VP, Xu C-Y, Li J (2014) Variations of annual and seasonal runoff in Guangdong Province, south China: spatiotemporal patterns and possible causes. Meteorol Atmos Phys 127:273–288

Zhao C, Mo D (2020) Holocene hydro-environmental evolution and its impacts on human occupation in Jianghan-Dongting Basin, middle reaches of the Yangtze River, China. J Geog Sci 30:423–438

Zheng W, Kuang A, Liu Z et al (2021) Analysing the spatial structure of urban growth across the Yangtze River Middle reaches urban agglomeration in China using NPP-VIIRS night-time lights data. GeoJournal 1–18

Zong Y, Chen X (1998) Flood on the Yangtze, China. Nat Hazards 22(2000):165–184